Journal of Solid State Chemistry 183 (2010) 2565–2569

Contents lists available at ScienceDirect

Journal of Solid State Chemistry

journal homepage: www.elsevier.com/locate/jssc

The kinetics of Al–Si spinel phase crystallization from calcined kaolin

Petr Ptáček*, František Šoukal, Tomáš Opravil, Magdaléna Nosková, Jaromír Havlica, Jiří Brandštetr

Centre for Materials Research, Faculty of Chemistry, Brno University of Technology, Purkyňova 464/118, Brno, CZ-612 00, Czech Republic

ARTICLE INFO

Article history:
Received 28 June 2010
Received in revised form
19 August 2010
Accepted 25 August 2010
Available online 8 September 2010

Keywords:
Al–Si spinel
Kaolin
Kaolinite
Heterogeneous kinetics
Thermal analysis

ABSTRACT

The crystallization of Al–Si spinel from medium ordered kaolin with high content of kaolinite was investigated using the differential thermal analysis (DTA). The apparent activation energy of the process was evaluated from the dependence of exothermic peak of crystallization on heating rate. Within the applied interval of heating rate (1–40 K min^{-1}) the temperature of peak maximum increases from initial value of 1220.5 K in about 54.2 K. The apparent activation energy of the process 856 ± 2 kJ $mol^{-1}$was calculated using the Kissinger equation. The growth morphology of Al–Si spinel crystal was evaluated from the Avrami parameter. The average value of morphology parameter determined within the observed interval of heating rate is 3.08 ± 0.03. This value indicates that crystallization mechanism of Al–Si spinel phase proceeds by bulk nucleation of the new phase with constant number of nuclei and that the three-dimensional growth of crystals is controlled by the reaction rate on the phases interface.

1. Introduction

Oxygen, silicon and alumina are essential constituents of the Earth's crust (82.5%) [1]. Minerals combined of these elements are silicates and aluminosilicates. With regard to this fact it is obvious that silicates and aluminosilicates belong to primary raw materials for industrial production. Ones of the most important raw materials—clay minerals played an important role during the development of human society. Originally the clays were used as building materials and for the production of ceramics and nowadays there is no industrial branch to be found where clay minerals or clay products are not applied. The current utilization of clays is summarized in publications [2,3].

Furthermore, the clay minerals cannot be supposed to lose their importance in the future; on the contrary: their significance will probably further increase. It was pointed out that clay minerals were supposed to be catalysts of reactions that led to the origin of life [4–7] which afterwards was developing in close contact with these materials. Thus the clays have no undesirable influence on living tissue. From this point of view the searching for the new applications of these materials is very desirable.

Clay minerals are aluminosilicates with layered structure where the individual layers are composed of two, three or four sheets. The sheets are formed either by tetrahedrons $[SiO_4]^{4-}$ and by octahedrons $[AlO_3(OH)_3]^{6-}$. The centre of tetrahedrons and octahedrons contains smaller metal cations and their apices are occupied with oxygen atoms or hydroxyl groups [3]. Clay minerals can be divided into seven groups. One of the most important clay minerals is the double-sheet phyllosilicate kaolinite ($Al_2Si_2O_5(OH)_4$) from the kaolinite and serpentine group [2].

Kaolinite is an essential component of kaolin. Beside the kaolinite a common kaolin contains accessory minerals, such as other phyllosilicates, feldspars, quartz, rutile, hematite, ilmenite, zircon, carbonates, sulphides and various kinds of ferrous and alumina hydroxides or oxo-hydroxides. The final composition of kaolinitic raw materials depends on the geological process which took place during weathering of parent rocks (mainly granite, rhyolite, syenite, trachyte, gneiss and arcose) [3,8–11].

The thermal reaction of kaolin group minerals was widely studied due to its industrial importance [12]. Four main thermally inducted processes take place during calcination of kaolinite: dehydroxylation of kaolinite to metakaolinite (Eq. 1), formation of Al–Si spinel phase from metakaolinite (Eq. 2), formation of mullite (Eq. 3) and crystallization of cristobalite from amorphous silica (Eq. 4) [11,13–15]

$$Al_2O_3\cdot 2SiO_2\cdot 2H_2O \xrightarrow{450-700\,^{\circ}C} Al_2O_3\cdot 2SiO_2 + 2H_2O_{(g)} \quad (1)$$

$$2(Al_2O_3\cdot 2SiO_2) \xrightarrow{925-1050\,^{\circ}C} 2Al_2O_3\cdot 3SiO_2 + SiO_{2(amorphous)} \quad (2)$$

$$3(2Al_2O_3\cdot 3SiO_2) \xrightarrow{\geq 1050\,^{\circ}C} 2(3Al_2O_3\cdot 2SiO_2) + 5SiO_2 \quad (3)$$

$$SiO_{2(amorphous)} \xrightarrow{\geq 1200\,^{\circ}C} SiO_{2(cristobalite)} \quad (4)$$

However, thermal decomposition of kaolinite to the thermodynamically stable phase, i.e. mullite and cristobalite, is much more complicated process than that one showed in the equations

* Corresponding author. Fax: +420 541 149 361.
E-mail address: ptacek@fch.vutbr.cz (P. Ptáček).

0022-4596/$ - see front matter © 2010 Elsevier Inc. All rights reserved.
doi:10.1016/j.jssc.2010.08.030

Nomenclature

E_A	apparent activation energy (kJ mol^{-1})
R^2	coefficient of determination
y	fractional conversion
T_i	extrapolated temperature of beginning of peak (K)
T_p	temperature of peak (K)
Θ	heating rate (K min^{-1})
W	width of peak (K)
$W_{1/2}$	half width of peak (K)
H	height of DTA peak (K mg^{-1})
R	universal gas constant (J K^{-1}mol^{-1})
n	growing parameter (Avrami parameter)

mentioned above. Removing of residual hydroxyls from metakaolinite [16], simultaneous formation of several phases and several mechanisms of formation of mullite [17] are the examples. In addition to the experimental conditions (heating rate, sample mass, applied experimental method…), the course of process is further influenced by many factors, e.g. the degree of disorder of kaolinite structure [15], pressure and partial water vapour pressure [18,19], heating rate [11,19], mechanical treatments and ultrasound processing of sample [20,21].

The aim of the paper is the investigation of formation kinetics of Al–Si spinel phase from calcined kaolin by differential thermal analysis. The activation energy of process is evaluated using Kissinger equation.

2. Experimental procedure

2.1. Kaolin

Washed kaolin Sedlec Ia from the Carlsbad region (Czech Republic) produced by the Sedlecký kaolin a.s. company was used for the study of thermal decomposition of kaolinite. This high quality kaolin, originally mined in open-cast mine near village Sedlec, has been commercially available since 1892 and it is often accepted to be the world's standard. The content of kaolinite guaranteed by producer is higher than 90 wt% with equivalent grain diameter median in the range 1.2–1.4 μm. The main impurities are mica group minerals and quartz. The colorant oxides content—hematite (α-Fe_2O_3) and tetragonal TiO_2 (rutile) is lower than 0.85 and 0.2 wt%, respectively. The characterization of initial state, properties and chemical composition of used kaolin were described in other papers. [22,23].

2.2. Differential thermal analysis

The 40 μm undersize of kaolin with the surface area of 20 m^2 g^{-1} (Chembet 3000) was used for the DTA experiments. The sample in the amount of 10 mg was introduced into Pt cup and arranged in a uniform layer. Further the crucible was inserted into TG-DTA analyzer Q600 (TA Instruments). The sample was heated upon the heating rate of 10 °C min^{-1} under flow of argon (100 cm^3 min^{-1}) to 1200 °C. DTA experiments were repeated six times (even more if needed) to obtain an average results without outlier values. The variation coefficient was lower than 1% for all sets of results.

2.3. Theory and applied mathematical background

Kissinger method, based on Eq. (5), is commonly used to analyze the kinetic process from DTA, DTG or DSC experiments [24–26]

$$\ln\left[\frac{\Theta}{T_p^2}\right] = \text{const.} - \frac{E_A}{RT_p} \tag{5}$$

where T_p is the maximum temperature of crystallization peak, Θ the applied heating rate and R universal gas constant. The Kissinger dependence can be used for direct calculation of activation energy from the changes of maximum of $\dot{y}$ vs.

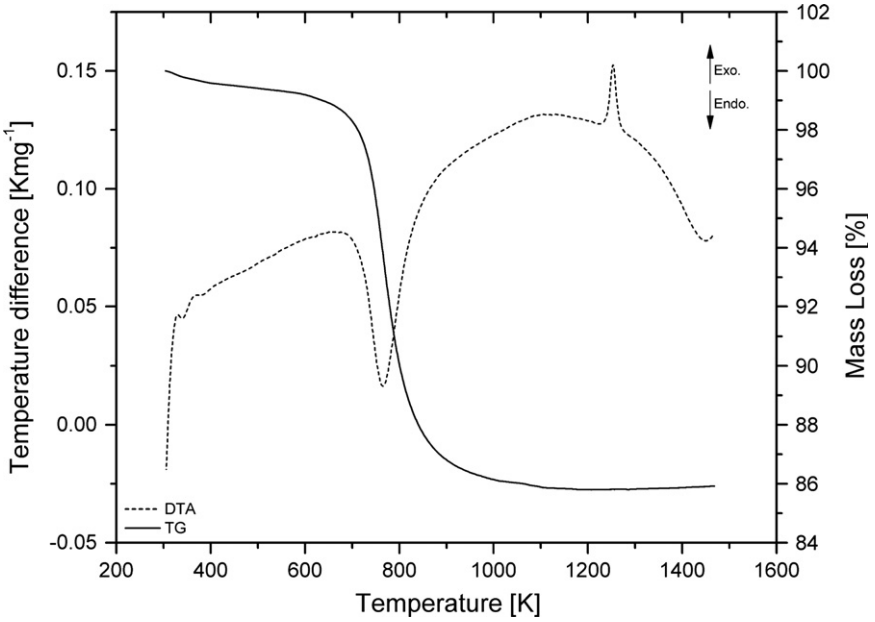

Fig.1. Simultaneous TG-DTA of kaolin for $\Theta = 10$ K min^{-1}.

temperature dependence with heating rate [26]. A plot of ln (Θ/T_p^2) vs. $1/T_p$ should give a straight line, which yields to the apparent activation energy of process (E_A). The detailed theory of the Kissinger approach is described in another publication. [27].

The crystallization mechanism can be determined from the shape factor (Avrami constant) n of the exothermic peak using Eq. (6) [28]

$$n = \frac{2.5}{w_{1/2}} \frac{T_p^2 R}{E_A} \tag{6}$$

where $w_{1/2}$ is the full width at half maximum (semi-breath) of the exothermic peak. For lower value of n surface crystallization mechanism is supposed rather than volume crystallization and/or the crystallization dimension is low. On the other hand, higher values of n are expected only in case of increasing nucleation rates, i.e. >2.5 in diffusion controlled reaction or >4 in polymorphic transformation.

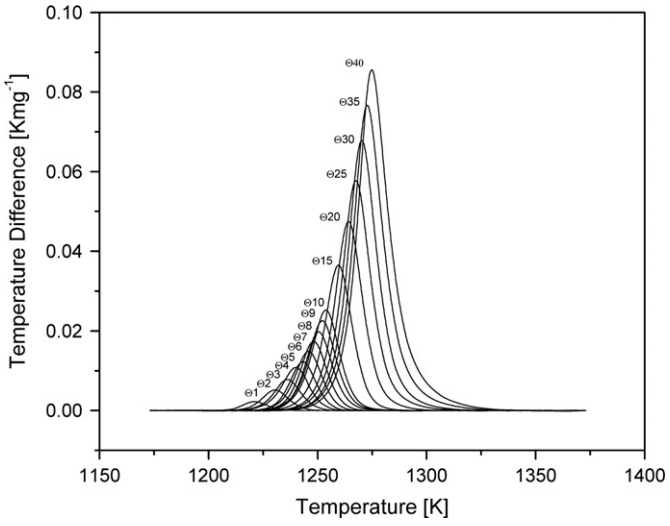

Fig.2. Influence of heating rate on the position of Al–Si spinel formation peak.

3. Results and discussion

The typical TG-DTA plot of kaolin heated to 1473 K using heating rate of 10 K min^{-1} is shown in Fig. 1.

Three endothermic and one exothermic peak appear on DTA curve. The thermogravimetric curve shows that endothermic processes are accompanied by the decrease of mass of the sample. The first inexpressive peak at 343 K pertains to the evaporation of water adsorbed on the surface. The mass of sample was reduced in about 0.3% during this process. A small weight loss of about 0.2 wt % that is adherent to the second endothermic peak at 385 K is probably caused by small amount of illite in kaolin (found by XRD [22]). Endothermic peak corresponding to the dehydroxylation of kaolinite (Eq. (1)) is located at 768 K. The mass of sample was reduced in about 12.8 wt% during this process.

Sharp exothermic peak at 1254 K is accompanied by the formation of the Al–Si spinel (Eq. (2)). The shift of the Al–Si spinel crystallization exothermic peak with heating rate is shown in Fig. 2. Table 1 provides information on the influence of increasing heating rate on pertinent parameters of peak.

Within the investigated interval of Θ (1–40 K min^{-1}) the value of T_p increases from initial 1220.5 to about 54.2 K. The increase of T_p with Θ conforms well to the following exponential law:

$$T_p = K\Theta^a \tag{7}$$

where constant K and a can be easily determined by linearization of experimental results. While constant K represents the peak maximum temperature for $\Theta=1$, the dimensionless coefficient a (scaling exponent) depends on the heat transport processes. It means that it is a function of many experimental parameters and state of sample. The logarithmic form of Eq. (7) ($\ln T_p - \ln \Theta$ plot) is shown in Fig. 3.

The values of K and a for investigated process of formation of Al–Si spinel were determined via linearization procedure to be 7.106 and 1.19×10^{-2}, respectively. The extrapolated beginning of peak (T_i) shows similar behaviour. On the other hand, the growth of height of peak shows almost linear dependency on Θ.

The Kissinger plot of $\ln(\Theta/T_p^2)$ vs. $1/T_p$ is shown in Fig.4. The apparent activation energy calculated from the slope is 856 ± 2 kJ mol^{-1}. Kinetic parameters of the formation of Al-Si

Table 1
Parameters of the Al–Si spinel crystallization DTA peak.

Heating rate	(K)				
(K min^{-1})	T_i	T_p	W	$W_{1/2}$	H ($\times10^{-3}$ K mg^{-1}]
1	1210.2 ± 0.2	1220.5 ± 0.3	22.1 ± 0.2	12.6 ± 0.2	2.3 ± 0.1
2	1219.2 ± 0.1	1230.5 ± 0.3	23.2 ± 0.1	13.7 ± 0.1	5.2 ± 0.1
3	1224.7 ± 0.3	1236.1 ± 0.3	24.0 ± 0.1	13.9 ± 0.1	7.8 ± 0.1
4	1227.1 ± 0.1	1239.4 ± 0.1	24.1 ± 0.1	13.9 ± 0.1	10.0 ± 0.2
5	1231.4 ± 0.2	1243.3 ± 0.1	23.8 ± 0.1	13.7 ± 0.1	12.3 ± 0.1
6	1233.3 ± 0.3	1245.3 ± 0.1	23.3 ± 0.1	13.9 ± 0.1	15.0 ± 0.1
7	1236.4 ± 0.1	1248.1 ± 0.1	23.9 ± 0.1	13.9 ± 0.1	17.2 ± 0.1
8	1238.3 ± 0.1	1250.2 ± 0.1	24.3 ± 0.1	14.2 ± 0.1	19.8 ± 0.2
9	1239.7 ± 0.1	1252.1 ± 0.1	24.6 ± 0.1	14.4 ± 0.1	21.9 ± 0.3
10	1241.1 ± 0.1	1253.6 ± 0.1	24.7 ± 0.1	14.5 ± 0.1	25.0 ± 0.2
15	1246.8 ± 0.1	1259.5 ± 0.1	25.4 ± 0.1	14.6 ± 0.1	36.6 ± 0.1
20	1251.6 ± 0.1	1264.0 ± 0.1	25.7 ± 0.1	14.8 ± 0.1	47.5 ± 0.3
25	1254.9 ± 0.1	1267.6 ± 0.1	26.5 ± 0.1	15.2 ± 0.1	57.8 ± 0.2
30	1257.5 ± 0.1	1270.3 ± 0.2	26.9 ± 0.1	15.3 ± 0.1	67.9 ± 0.2
35	1260.0 ± 0.1	1272.8 ± 0.2	27.6 ± 0.1	15.7 ± 0.1	76.8 ± 0.3
40	1262.1 ± 0.1	1274.7 ± 0.2	28.1 ± 0.1	16.1 ± 0.1	85.7 ± 0.6

T_i is the extrapolated temperature of beginning of peak.
T_p is the temperature of peak.
W is the peak width, the difference between extrapolated temperature of beginning and the end of peak.
$W_{1/2}$ is the peaks half width.
H is the peaks height.

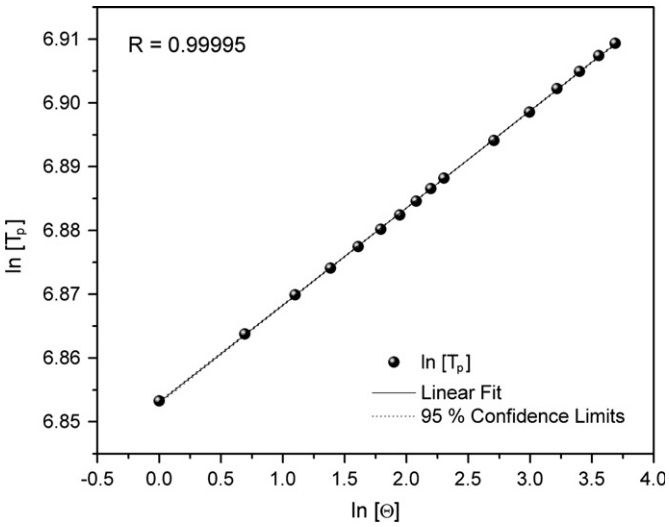

Fig.3. Dependence of position of peak (T_p) on heating rate.

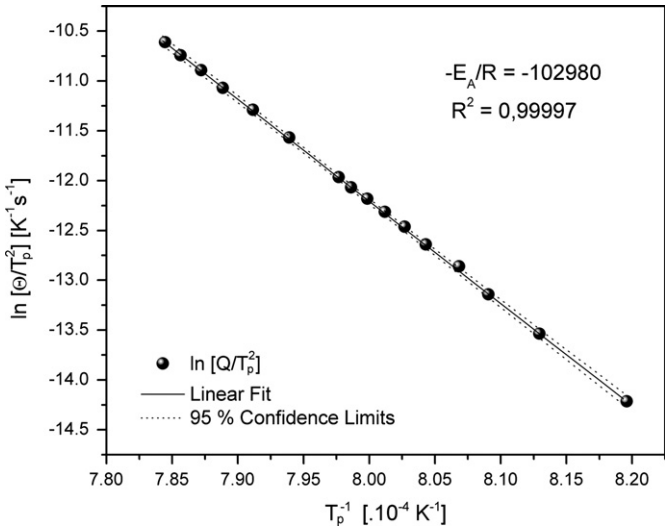

Fig.4. Kissinger plot for the formation of Al–Si spinel.

Table 2
Kinetic parameters of the formation of Al–Si spinel and specification of mechanism of crystallization.

Heating rate (K min^{-1})	T_p^{-1} ($\times 10^{-4}$ K^{-1})	-ln(ΘT_p^{-2})	Avrami constant
1	8.1959	−14.2134	3.5
2	8.1294	−13.5366	3.2
3	8.0906	−13.1407	3.2
4	80619	−12.8601	3.2
5	8.0388	−12.6427	3.2
6	8.0261	−12.4635	3.2
7	8.0119	−12.3129	3.2
8	7.9984	−12.1828	3.1
9	7.9862	−12.0680	3.1
10	7.9758	−11.9653	3.1
15	7.9392	−11.5690	3.0
20	7.9114	−11.2883	3.0
25	7.8886	−11.0710	2.9
30	7.8721	−10.8928	2.9
35	7.8565	−10.7426	2.8
40	7.8447	−10.6121	2.7

spinel from heated kaolin and the values of Avrami factor are calculated from Eq. (6) and are listed in Table 2.

The average value of the growth morphology parameter within studied interval of heating rate is 3.08 ± 0.03. It indicates instantaneous bulk nucleation of spinel phase and subsequent three-dimensional growth of nuclei. The growth of nuclei is controlled by the rate of reaction on the interface of phases.

4. Conclusion

Crystallization and growth mechanism of Al–Si spinel in thermally treated kaolin were studied using differential thermal analysis. Temperature of crystallization of Al–Si spinel increases with heating rate from initial 1220.5 K measured at Θ 1 K min^{-1} up to 1274.7 K measured at Θ 40 K min^{-1}, i.e. the temperature of the process increases in 54.2 K. The apparent activation energy of process was calculated by Kissinger equation to be 856 ± 2 kJ mol^{-1}. The average value of the growth morphology (Avrami) parameter is 3.08 ± 0.03. Therefore bulk instantaneous nucleation of spinel phase and subsequent three-dimensional growth of nuclei are supposed. Subsequent three-dimensional growth of crystals is controlled by the rate of reaction on the interface of phases. Experimental dependence of T_p on Θ shows that the rate of the process is decreasing with growing value of heating rate.

Acknowledgments

This paper arose of the research project supported by the Ministry of Education, Youth and Sports No. 2B08024 and Project no. CZ.1.05/2.1.00/01.0012 "Centres for Materials Research at FCH BUT" supported by operational program Research and Development for Innovations.

References

[1] Frederick K. Lutgens, Tarbuck Edward J., in: Essentials of Geology, 7th Ed., Prentice Hall, 2000.
[2] H.H. Murray, Applied Clay Science 17 (2000) 207–221.
[3] J. Konta, Applied Clay Science 10 (1995) 275–335.
[4] J.T. Trevors, Research in Microbiology 153 (2002) 487–491.
[5] J.H. McClendon, Earth-Science Reviews 47 (1999) 71–93.
[6] C. de Sousa, F. Gomes, J.B.P. Silva, Applied Clay Science 36 (2007) 4–21.
[7] A.E. Lyubarev, B.I. Kurganov, BioSystems 42 (1997) 103–110.
[8] M.D.C. Santos, A.F.D.C. Varajão, J. Yvon, Journal of Geochemical Exploration 88 (2006) 318–320.
[9] J. Sei, F. Morato, G. Kra, S. Staunton, H. Quiquampoix, J.C. Jumas, J. Olivier-Fourcade, Journal of African Earth Sciences 46 (2006) 245–252.
[10] M.L. da Costa, D.J.L. Sousa, R.S. Angélica, Journal of South American Earth Sciences 27 (2009) 219–234.
[11] O. Castelein, B. Soulestin, J.P. Bonnet, P. Blanchart, Ceramic International 27 (2001) 517–522.
[12] R.M.T. Sánchez, E.I. Basaldella, J.F. Marco, Journal of Colloid and Interface Science 215 (1999) 339–344.
[13] Y.-F. Chen, M.-Ch Wang, M.-H. Hon, Journal of the European Ceramic Society 24 (2004) 2389–2397.
[14] R.L. Frost, E. Horváth, É. Makó, J. Kristóf, Á. Rédey, Thermochimica Acta 408 (2003) 103–113.
[15] K. Heide, M. Földvari, Thermochimica Acta 446 (2006) 106–112.
[16] V. Balek, M. Murat, Thermochimica Acta 282–283 (1996) 385–397.
[17] A.K. Chakraborty, Thermochimica Acta 398 (2003) 203–209.
[18] J. Temuujin, K. Okada, K.J.D. MacKenzie, Ts. Jadambaa, Journal of the European Ceramic Society 19 (1999) 105–112.
[19] K. Nahdi, P. Llewellyn, F. Rouquérol, J. Rouquérol, N.K. Ariguib, M.T. Ayedi, Thermochimica Acta 390 (2002) 123–132.
[20] C. Vizcayno, R. Castelló, I. Ranz, B. Calvo, Thermochimica Acta 428 (2005) 173–183.
[21] J.L. Pérez-Rodríguez, J. Pascual, F. Franco, M.C. Jiménez de Haro, A. Duran, V. Ramírez del Valle, L.A. Pérez-Maqueda, Journal of the European Ceramic Society 26 (2006) 74–753.
[22] P. Ptáček, D. Kubátová, J. Havlica, J. Brandštetr, F. Šoukal, T. Opravil, Thermochimica Acta 501 (2010) 24–29.

[23] P. Ptáček, D. Kubátová, J. Havlica, J. Brandštetr, F. Šoukal, T. Opravil, The non-isothermal kinetics analysis of the thermal decomposition of kaolinite by thermogravimetric analysis, Powder Technology, doi:10.1016/j.powtec.2010.08.004.
[24] M. Romero, J. Martín-Márquez, J Ma., Journal of the European Ceramic Society 26 (2006) 1647–1652.
[25] D. Prodanović, Ž.B. Živković, S. Radosavljević, Applied Clay Science 12 (1997) 267–274.
[26] J. Šesták, in: Thermal Analysis Part D, Volume XII D: Thermophysical Properties of Solids Their Measurement and Theoretical Thermal Analysis (Comprehensive Analytical Chemistry), Elsevier Science, 1984 ISBN-10: 0-444-99653-2.
[27] H.E. Kissinger, Analytical Chemistry 29 (1959) 1702.
[28] T. Takei, Y. Kameshima, A. Yasumori, K. Okada, Journal of the European Ceramic Society 21 (2001) 2487–2493.